

# On the Efficiency of Disorder-induced Heating of Ultracold Plasmas

Yurii V. Dumin<sup>1,2, a)</sup> and Anastasiia T. Lukashenko<sup>3, b)</sup>

<sup>1)</sup>*Lomonosov Moscow State University, Sternberg Astronomical Institute,  
Universitetskii prosp. 13, 119234 Moscow, Russia*

<sup>2)</sup>*Space Research Institute of Russian Academy of Sciences,  
Profsoyuznaya str. 84/32, 117997 Moscow, Russia*

<sup>3)</sup>*Lomonosov Moscow State University, Skobeltsyn Institute of Nuclear Physics,  
Leninskie gory, GSP-1, 119991 Moscow, Russia*

Starting from the beginning of their research in the early 2000's, the ultracold plasmas were considered as a promising tool to achieve considerable values of the Coulomb coupling parameter for electrons. Unfortunately, this was found to be precluded by a sharp spontaneous increase of temperature, which was commonly attributed to the so-called disorder-induced heating (DIH). It is the aim of the present paper to quantify this effect as function of the initial ionic disorder and, thereby, to estimate the efficiency of its mitigation, *e.g.*, by the Rydberg blockade. As a result of the performed simulations, we found that the dynamics of electrons exhibited a well-expressed transition from the case of the quasi-regular arrangement of ions to the disordered one; the magnitude of the effect being about 30%. Thereby, we can conclude that the two-step formation of ultracold plasmas—involving the intermediate stage of the blocked Rydberg gas—can really serve as a tool to increase the degree of Coulomb coupling, but the efficiency of this method is moderate.

PACS numbers: 52.25.Kn, 52.27.Gr, 52.65.Yy

## I. INTRODUCTION

The so-called ultracold plasmas are neutral systems of charged particles with typical electronic temperatures from a few to several tens of Kelvin, which are obtained by a photoionization of gases cooled in the magneto-optical traps; *e.g.*, reviews<sup>1–4</sup>. The experimental realization of such plasmas became feasible in the very late 1990's and early 2000's, and they opened a new area of research in the non-ideal plasma physics<sup>5,6</sup>.

It was initially expected that the extremely high values of the Coulomb coupling parameter

$$\Gamma_e \approx \frac{\langle U \rangle}{\langle K \rangle} \quad (1)$$

(where  $K$  and  $U$  are the kinetic and potential energies of an electron) can be achieved in this way. Really, if energy of the ionizing laser irradiation was chosen to be slightly above the ionization threshold of the cold neutral atoms, the initial kinetic energy of the released electrons would be very low. Therefore, it was expected in the first experiments<sup>7</sup> that very large values of the coupling parameter (1) could be obtained, *e.g.*, tens or hundreds. Unfortunately, it was quickly recognized that the situation is not so simple: In fact, the cold photoelectrons are quickly accelerated by the electric fields of nearby ions, and their temperature spontaneously increase by many times.

A simple pictorial explanation of this effect is the so-called disorder-induced heating (DIH)<sup>8</sup>: The charged particles (firstly, electrons and, at the longer time scale, also the

ions) tend to move to the positions with minimal potential energy. As a result, since the total energy of the system should be conserved, a kinetic energy of the particles will increase. Therefore, DIH looks like the unavoidable effect, limiting the temperature from below.

However, it was suggested by the same authors<sup>8</sup> that one can get around the DIH effect by preparation of the system of charged particles in the “correlated” state with a reduced Coulomb energy. A particular realization of this approach was implemented a decade later in the work<sup>9</sup>: Namely, the cold neutral atoms were initially transferred to the state of the Rydberg blockade, when the already excited atoms—due to their strong electric fields—shift the energy levels of the nearby atoms, thereby prohibiting their excitation to the same Rydberg state<sup>10–12</sup>. As a result, a quasi-regular arrangement of the excited atoms is formed, where their close location to each other is excluded (*e.g.*, Fig. 3 in paper<sup>13</sup>). Next, after the photoionization of Rydberg atoms, the resulting ions will also be well separated from each other. Therefore, one can expect that DIH will no longer take place, because the system of ions is already in the “quasi-crystalline” state with a minimal potential energy.

The experiment<sup>9</sup> was really able to trace the plasma formation from the blocked Rydberg gas, but it remained unclear if the resulting electron temperature was appreciably reduced (and, respectively, the Coulomb coupling parameter increased). This was caused, firstly, by the fact that the ionization proceeded mostly by the spontaneous avalanche process (and, therefore, did not strictly preserve the initial quasi-crystalline arrangement of the Rydberg atoms) and, secondly, by the insufficient diagnostic capabilities to measure the electron temperature (S. Whitlock, private communication). Besides, there was no a clear theoretical prediction how much could be the magnitude of the expected reduction in temperature. Surprisingly, while the DIH mechanism was discussed for the first time about 20 years ago<sup>8</sup>, it was subsequently stud-

<sup>a)</sup>Corresponding author's electronic mail:  
dumin@pks.mpg.de, dumin@yahoo.com

<sup>b)</sup>Electronic mail: lukashenko@dec1.sinp.msu.ru, a\_lu@mail.ru

ied mostly for ions<sup>14–18</sup>, and there are no reliable calculations of its influence on the electron temperature till now.

So, it is the aim of the present paper to quantify the DIH effect in electrons as function of the initial disorder. In fact, this problem was partially touched in our previous work about the clusterized plasmas<sup>13</sup>. As a particular case of the non-trivial arrangement of the background ions, we considered there also their quasi-regular distribution and found that the resulting electron temperature was somewhat reduced. However, the degree of such a reduction was comparable to the uncertainty (r.m.s. variation) of that simulations. Besides, it remained unclear how the corresponding effect depends on the degree of disorder and, particularly, how it tends to the purely random case when the disorder becomes sufficiently large. In the present work—due to much better accuracy of the simulations—all these issues will be resolved.

## II. NUMERICAL MODEL

A quite general model of ionic background with different degrees of disorder can be formulated by the following way: Let us consider initially a perfect cubic lattice of ions. The size of its cell  $l$  will be used from here on as the unit of length, and all the distances will be normalized respectively. Next, let each ion be shifted from its original position by a distance given by the normal (Gaussian) distribution with r.m.s. deviation  $\sigma_{\text{reg}}$ , as illustrated in the bottom row of Fig. 1. Then, at  $\sigma_{\text{reg}} \ll 1$  (in dimensionless units) the ionic distribution is quasi-regular; but it becomes more and more disordered when  $\sigma_{\text{reg}}$  increases; and finally, at  $\sigma_{\text{reg}} \sim 1$ , we evidently get a completely random distribution.

These features are well expressed in the histograms of interparticle separation (or, up to normalization, the two-point correlation functions) shown in the top row of Fig. 1. Really, at  $\sigma_{\text{reg}} \ll 1$  one can see a series of sharp peaks, which represent a set of the preferable interparticle distances in the quasi-regular lattice. Next, when the disorder increases, these peaks are gradually smoothed out; and finally, at  $\sigma_{\text{reg}} \sim 1$ , the histograms take the Gaussian shape, which is typical for random distributions.

To study dynamics of the electrons against the above-mentioned kinds of ionic background, we shall numerically integrate their equations of motion:

$$\frac{d^2 \mathbf{r}_i}{dt^2} = - \sum_j e^2 \frac{\mathbf{r}_i - \mathbf{R}_j}{|\mathbf{r}_i - \mathbf{R}_j|^3} + \sum_{k \neq i} e^2 \frac{\mathbf{r}_i - \mathbf{r}_k}{|\mathbf{r}_i - \mathbf{r}_k|^3}, \quad (2)$$

where  $\mathbf{r}_i$  and  $\mathbf{R}_i$  are the electronic and ionic coordinates, respectively; and  $e$  is the electron charge. The ions are assumed to be immobile, because we are interested only in the sufficiently short time intervals. The initial electron coordinates  $\mathbf{r}_i(0)$  are given by the uniform statistical distribution; and their initial velocities  $\mathbf{v}_i(0)$ , by the normal (Maxwellian) law with the r.m.s. variation  $\hat{\alpha}_v$ .

Strictly speaking, the initial values of the electron coordinates and velocities strongly depend on the details of the ionization process. For example, in the case of instantaneous

photoionization, the initial electron positions will be strongly correlated with the positions of ions<sup>19</sup>, while distribution of the electron velocities will look like the delta-function. However, if the photoionization takes some time, the released electrons should be mixed between the ions and the distribution of their velocities smoothed out, resulting in the Maxwellian form.

Next, we shall use the perfectly reflective boundary conditions, and the Coulomb interactions will be calculated within the fixed simulation box. An alternative choice—used in the most of the previous works on the ultracold plasmas—is to employ the periodic boundary conditions, when a particle leaving the simulation box through one of its boundaries simultaneously enters it through the opposite boundary. The Coulomb interactions are usually calculated in such a case by the “wrapping” algorithm<sup>19</sup>, when each particle interacts with other particles within a moving cube of size  $\pm L/2$ , centered at that particle (where  $L$  is the total size of the simulation box). In principle, none of these options is perfect: The reflective boundaries evidently affect the bulk properties of the plasmas. On the other hand, the periodic boundary conditions with the wrapping procedure, at the first sight, avoid this problem. However, a closer inspection shows that swapping of a charged particle between the boundaries of the moving box results in the abrupt unphysical changes in the direction of Coulomb forces between the pair of particles. From this point of view, the reflective boundaries look better because their effect on the bulk properties has a clear physical meaning<sup>20</sup>, and it will evidently disappear with increasing the number of particles.

Besides, in the context of our simulations, the decisive advantage of the reflective boundary conditions is that they are well consistent with the algorithms of numerical integration with the adaptive stepsize control, such as the subroutines `odeint`, `rkck`, and `rkqs` from the Numerical Recipes<sup>21</sup>. These subroutines were used in our previous work<sup>13</sup> and demonstrated a beautiful performance. Particularly, they are able to work with the “true” (singular) Coulomb potentials, without a need for their cut-off or “softening” at the small distances. This excludes any artifacts caused by the distorted potentials. (Let us mention that dealing with such potentials without the adaptive stepsize control would require the huge computational resources<sup>22</sup>.)

All the results will be presented below in the dimensionless units, normalized by the following way: the unit of length is the mean distance between the ions  $l$  (the corresponding unitary cells are marked by dotted lines in Fig. 1); the unit of time, up to numerical factor on the order of unity, is the inverse plasma frequency,  $\tau = \sqrt{m l^3 / e^2} = \sqrt{4\pi} / \omega_{p1}$ ; and the unit of energy is the characteristic Coulomb energy at the interparticle distance,  $U = e^2 / l$ . The dimensionless quantities, expressed in the above-mentioned units, will be denoted by hats.

Next, the electron temperature is assumed to be related to the kinetic energy per electron by the same formula as for an ideal gas,  $T_e = (2/3) K / k_B$ . Although we deal here with a substantially non-ideal case, it was found in paper<sup>19</sup> that such definition reasonably agrees with a more elaborated derivation

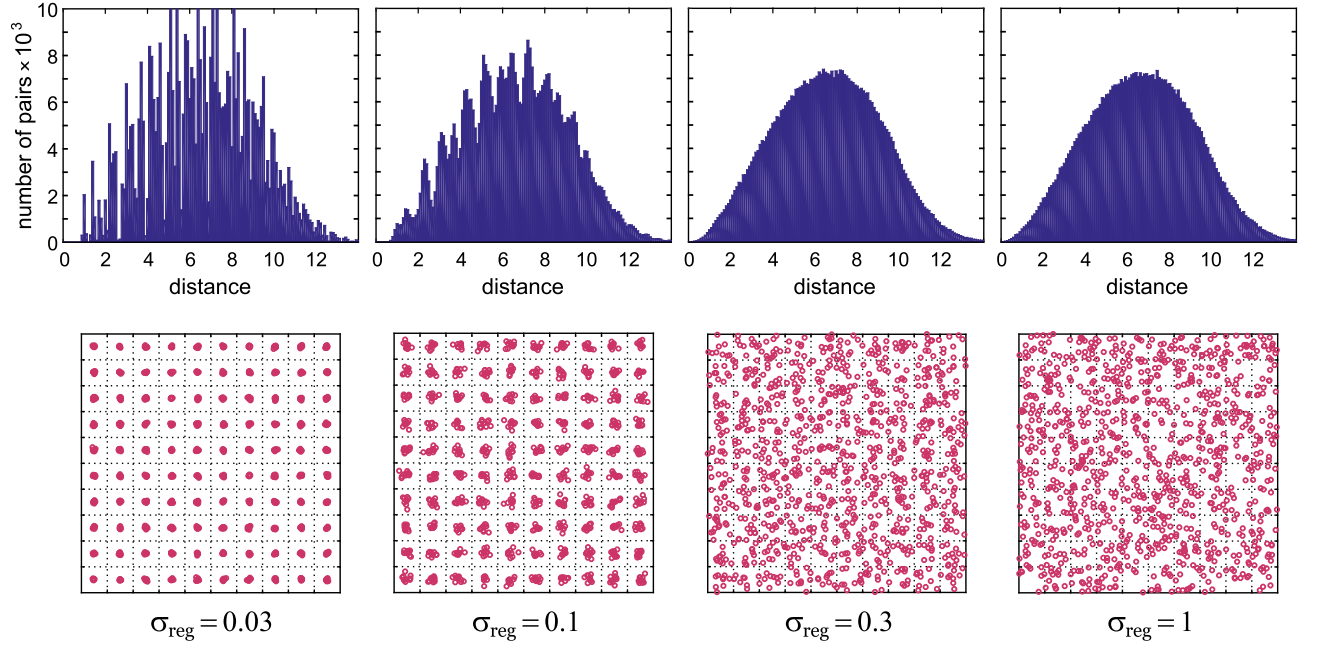


FIG. 1. Examples of the ionic arrangement in the  $xy$ -plane (bottom row) and the corresponding histograms of the interparticle separation (top row) for the quasi-regular distributions with different degree of disorder  $\sigma_{\text{reg}}$ . For convenience, a grid of the dotted lines illustrates a characteristic space per one particle in the perfect cubic lattice.

of  $T_e$ , based on the approximation of the simulated velocity distributions by the Maxwellian ones. A theoretical explanation of this fact can be found in paper<sup>23</sup>.

### III. RESULTS OF THE SIMULATIONS

Our simulations were performed for the system of 1000 particles of each kind (electrons and ions), *i.e.*, the simulated volume was composed of  $10 \times 10 \times 10$  unitary cells, as depicted in Fig. 1. This is 8 times greater than in our previous simulations of the clusterized plasmas<sup>13</sup>: since influence of the quasi-regular ionic arrangement is a finer effect, we had to increase the number of simulated particles.

In the particular case presented below we used  $\hat{\sigma}_v = 0.3$ , which implies that the initial kinetic energy of electrons was about an order of magnitude less than their potential (Coulomb) energy. In other words, the plasma was already in the non-ideal state, and our aim was to check if this state will survive against the disorder-induced heating.

The simulations were performed for the following degrees of disorder:  $\sigma_{\text{reg}} = 0.01, 0.03, 0.1, 0.3, 1$  and 3, as well as for the purely random ionic distribution. To get the statistically significant results, five versions of initial conditions—randomly generated both for the ions and electrons—were used for each of these values. Despite dealing with singular interparticle potentials, the algorithm of the adaptive stepsize control enabled us to get a sufficiently high accuracy of integration (estimated, as usual, by the conservation of the total energy). In the worst case it was 1.4%, but usually by one or two orders of magnitude better.

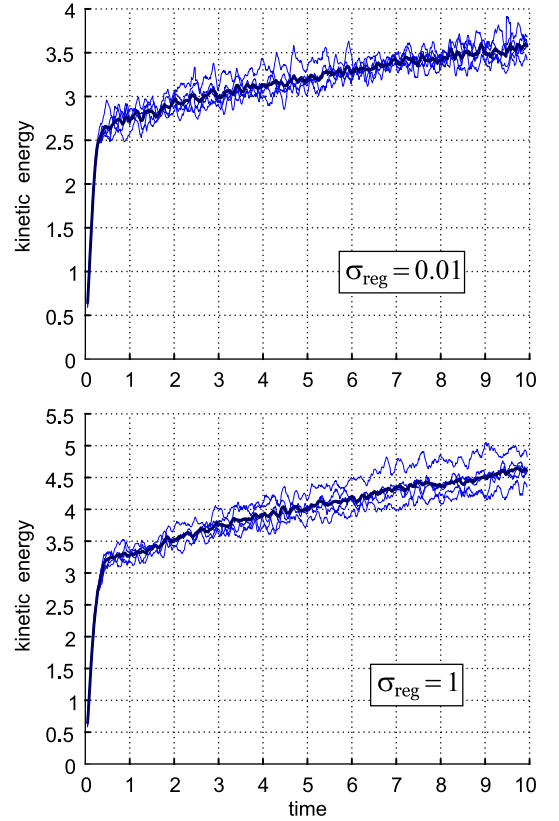


FIG. 2. The individual profiles of the electron kinetic energy as function of time (thin curves) and their average behavior (thick curves) at  $\sigma_{\text{reg}} = 0.01$  and 1 (top and bottom panels, respectively).

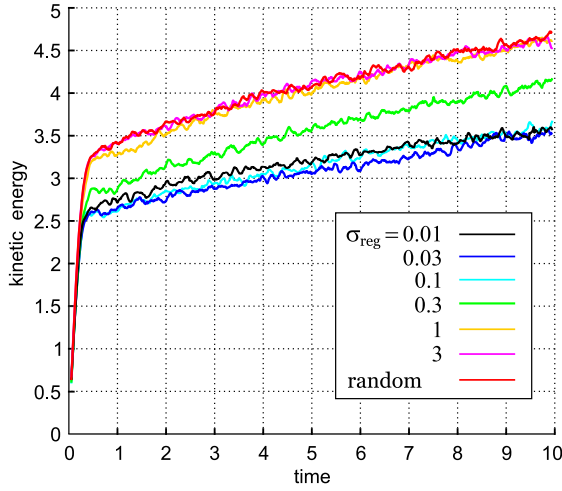


FIG. 3. The average (over 5 realizations) temporal profiles of the electron kinetic energy  $\langle \hat{K} \rangle$  for the entire set of the disorder parameters  $\sigma_{\text{reg}}$ .

Examples of the simulated temporal behavior of the dimensionless kinetic energy of electrons are presented in Fig. 2. To avoid obscuring the plots with a lot of sharp peaks, caused by the interparticle collisions, they were smoothed out over a running window of width  $\Delta t = 0.1$ . In principle, the general shape of these curves—a quick initial jump at the timescale  $\hat{t} \approx 0.5$  followed by a much longer gradual increase—is well known already from the pioneering work by Kuzmin and O’Neil<sup>24</sup>. It is the aim of our study to reveal their dependence on the arrangement of the ionic background.

Figure 3 shows the average temporal dependences of the electron kinetic energy for the entire variety of the disorder parameters  $\sigma_{\text{reg}}$ , ranging from an almost perfect ionic lattice to the completely random distribution. One can see here three types of the curves: Type I corresponds to the small values of  $\sigma_{\text{reg}}$  (0.01, 0.03, and 0.1), *i.e.*, the weakly distorted lattices. Type II with  $\sigma_{\text{reg}} = 0.3$  is the intermediate case, corresponding to the moderately distorted lattice. At last, the curves of Type III belong either to the cases of strongly distorted lattice,  $\sigma_{\text{reg}} = 1$  and 3, or to the completely random distribution. As could be naturally expected, just the Type II indicates a noticeable change in the temporal behavior of the electron kinetic energy  $\langle \hat{K} \rangle$ . Namely, when  $\sigma_{\text{reg}}$  increases, the initial jump (at the timescale  $0 \leq \hat{t} \lesssim 0.5$ ) becomes more pronounced. The subsequent gradual increase in  $\langle \hat{K} \rangle$  at  $\hat{t} \gtrsim 0.5$ , in principle, also changes but insignificantly.

Referring to the histograms of the interparticle separation, presented in the top row of Fig. 1, one can see that at small values of  $\sigma_{\text{reg}}$  (*e.g.*, 0.03 and 0.1) they exhibit a series of sharp peaks, which are typical for the crystalline-like structures. On the other hand, at the large values of  $\sigma_{\text{reg}}$  (*e.g.*, 1) their shape closely resembles the purely-random Gaussian one. It is interesting that in the intermediate case  $\sigma_{\text{reg}} = 0.3$  the histogram is almost Gaussian, but the curve  $\langle \hat{K} \rangle(\hat{t})$  in Fig. 3 exhibits a clearly distinct behavior. In fact, a closer inspection of the patterns of ionic arrangement in the bottom row of Fig. 1 shows

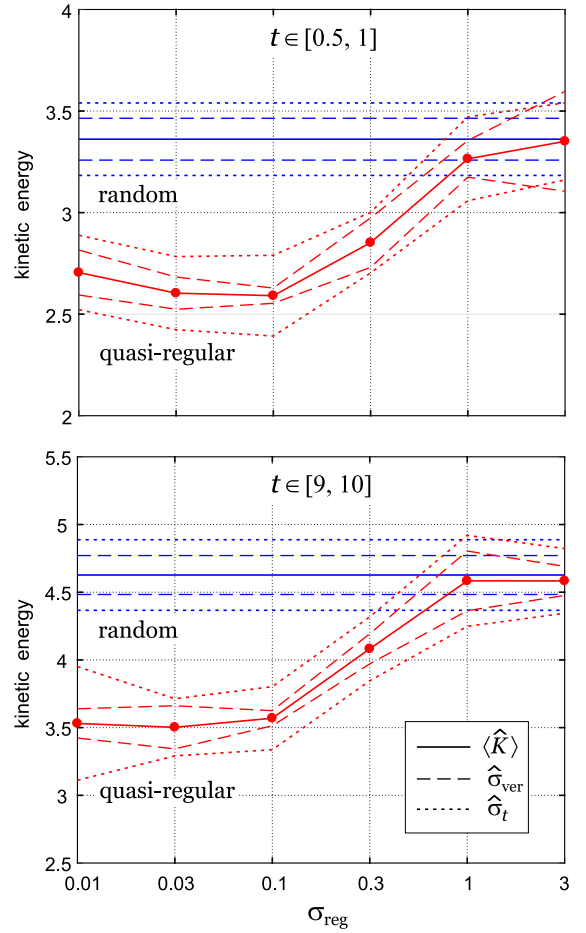


FIG. 4. Average values of the electron kinetic energy established at the time intervals  $[0.5, 1]$  (top panel) and  $[9, 10]$  (bottom panel), as well as their r.m.s. deviations, as functions of the disorder parameter  $\sigma_{\text{reg}}$ .

that the case  $\sigma_{\text{reg}} = 0.3$  preserves some features of the quasi-regularity: namely, there are no occasional “voids”, typical for the random distributions.

To quantify three above-mentioned types of the temporal behavior  $\langle \hat{K} \rangle(\hat{t})$ , we calculated the average values of the electron kinetic energy at two time intervals:  $\hat{t} \in [0.5, 1]$  and  $\hat{t} \in [9, 10]$ . The first of these quantities characterizes a magnitude of the initial jump of  $\hat{K}$ , which was often attributed just to the disorder-induced heating; while the second quantity represents the total increase in  $\hat{K}$  after a sufficiently long period of evolution, which includes also the subsequent heating of plasma due to recombination. Both these quantities are presented in Fig. 4 as functions of  $\sigma_{\text{reg}}$ .

To estimate a statistical significance of the simulations, we plotted in this figure also the r.m.s. variations of the average energy with respect to various versions of the initial conditions  $\hat{\sigma}_{\text{ver}}$  and with respect to time  $\hat{\sigma}_t$  (over the corresponding time intervals). These quantities are shown by the dashed and dotted lines, respectively. As is seen,  $\hat{\sigma}_{\text{ver}}$  is appreciably smaller than  $\hat{\sigma}_t$ . In other words, five versions of the initial conditions are quite sufficient. On the other hand, the tempo-

ral r.m.s. variation  $\hat{\sigma}_r$  is evidently unavoidable, and its effect can be reduced only by increasing the number of particles in the simulated system.

#### IV. DISCUSSION AND CONCLUSIONS

The main result of our study is the identification of the clear transition of the electron dynamics from the case of quasi-regular ionic background (*e.g.*, caused by the Rydberg blockade, as discussed in the Introduction) to the random one. Let us mention that some reduction of the electron temperature in the regularized ionic arrangement was detected already in our previous study<sup>13</sup>, but this effect in  $\hat{K}(\hat{t})$  was comparable to the uncertainties  $\hat{\sigma}_{\text{ver}}$  and  $\hat{\sigma}_r$ ; see Table 1 and Fig. 8 in that paper. Besides, it was rather surprising why there was no a clear transition of  $\hat{K}(\hat{t})$  to the purely random case when  $\sigma_{\text{reg}}$  tended to unity. In the present study—due to the enhanced accuracy of simulations—this puzzle was resolved, and the clear transition was identified.

Unfortunately, the effect of reduction of the electron temperature was found to be not so large: as is seen in Fig. 4, it is approximately 30% both immediately after the sharp jump, occurring at the timescale of one dimensionless unit (*i.e.*, about the inverse plasma frequency) and at the longer time interval, when a heat release due to recombination comes into play. It is interesting to mention that yet another method to reduce the electron temperature (and, thereby, to increase the Coulomb coupling parameter) was suggested in papers<sup>25,26</sup>. This is adding the Rydberg atoms with binding energies  $|E_b| \lesssim (2-3)k_B T_e$  into the ultracold plasmas. As a result, their inelastic collisions with free electrons will lead to a further excitation of the atoms and cooling of the electrons. It was found in the above-cited papers that the overall efficiency of such a process should be about 20–30%, *i.e.*, actually the same as in the method based on the Rydberg blockade<sup>9</sup>.

#### ACKNOWLEDGMENTS

YVD is grateful to J.-M. Rost and S. Whitlock for stimulating this study, as well as to A.A. Bobrov, S.A. Mayorov, U. Saalman, and V.S. Vorob'ev for fruitful discussions and valuable suggestions.

#### AUTHOR DECLARATIONS

##### Conflict of Interest

The authors have no conflicts to disclose.

#### Author Contributions

YVD suggested the theoretical concept, developed the corresponding software, and prepared the manuscript; both authors performed the simulations and analyzed the obtained results.

#### DATA AVAILABILITY

The data that support the findings of this study are available from the corresponding author upon reasonable request.

#### References:

- <sup>1</sup>P. Gould and E. Eyster, *Phys. World* **14**(3), 19 (2001).
- <sup>2</sup>S. Bergeson and T. Killian, *Phys. World* **16**(2), 37 (2003).
- <sup>3</sup>T. Killian, *Science* **316**, 705 (2007).
- <sup>4</sup>T. Killian, T. Pattard, T. Pohl, and J. Rost, *Phys. Rep.* **449**, 77 (2007).
- <sup>5</sup>S. Ichimaru, *Rev. Mod. Phys.* **54**, 1017 (1982).
- <sup>6</sup>V. Fortov and I. Iakubov, *The Physics of Non-ideal Plasma* (World Sci., Singapore, 2000).
- <sup>7</sup>T. Killian, S. Kulin, S. Bergeson, L. Orozco, C. Orzel, and S. Rolston, *Phys. Rev. Lett.* **83**, 4776 (1999).
- <sup>8</sup>D. Gericke and M. Murillo, *Contrib. Plas. Phys.* **43**, 298 (2003).
- <sup>9</sup>M. Robert-de Saint-Vincent, C. Hofmann, H. Schempp, G. Günter, S. Whitlock, and M. Weidemüller, *Phys. Rev. Lett.* **110**, 045004 (2013).
- <sup>10</sup>M. Lukin, M. Fleischhauer, R. Cote, L. Duan, D. Jaksch, J. Cirac, and P. Zoller, *Phys. Rev. Lett.* **87**, 037901 (2001).
- <sup>11</sup>D. Tong, S. Farooqi, J. Stanojevic, S. Krishnan, Y. Zhang, R. Côté, E. Eyster, and P. Gould, *Phys. Rev. Lett.* **93**, 063001 (2004).
- <sup>12</sup>K. Singer, M. Reetz-Lamour, T. Amthor, L. Gustavo Marcassa, and M. Weidemüller, *Phys. Rev. Lett.* **93**, 163001 (2004).
- <sup>13</sup>Y. Dumin and A. Lukashenko, *Phys. Plas.* **29**, 113506 (2022).
- <sup>14</sup>T. Pohl, T. Pattard, and J. Rost, *J. Phys. B* **37**, L183 (2004).
- <sup>15</sup>T. Pohl, T. Pattard, and J. Rost, *Phys. Rev. Lett.* **94**, 205003 (2005).
- <sup>16</sup>Z. Donkó, *J. Phys. A* **42**, 214029 (2009).
- <sup>17</sup>D. Murphy, R. Scholten, and B. Sparkes, *Phys. Rev. Lett.* **115**, 214802 (2015).
- <sup>18</sup>D. Murphy and B. Sparkes, *Phys. Rev. E* **94**, 021201(R) (2016).
- <sup>19</sup>K. Niffenegger, K. Gilmore, and F. Robicheaux, *J. Phys. B* **44**, 145701 (2011).
- <sup>20</sup>S. Mayorov, A. Tkachev, and S. Yakovlenko, *Physics–Uspekhi* **37**, 279 (1994).
- <sup>21</sup>W. Press, S. Teukolsky, W. Vetterling, and B. Flannery, *Numerical Recipes in Fortran 77: The Art of Scientific Computing*, vol. 1 (Cambridge Univ. Press, Cambridge, UK, 1992), 2nd ed.
- <sup>22</sup>Y. Dumin, *Plas. Phys. Rep.* **37**, 858 (2011).
- <sup>23</sup>Y. Dumin, *J. Low Temp. Phys.* **119**, 377 (2000).
- <sup>24</sup>S. Kuzmin and T. O'Neil, *Phys. Rev. Lett.* **88**, 065003 (2002).
- <sup>25</sup>N. Vanhaecke, D. Comparat, D. Tate, and P. Pillet, *Phys. Rev. A* **71**, 013416 (2005).
- <sup>26</sup>E. Crockett, R. Newell, F. Robicheaux, and D. Tate, *Phys. Rev. A* **98**, 043431 (2018).